Solar Physics (2005) 232: 41–62

THE PARKER PROBLEM AND THE THEORY OF CORONAL HEATING

I. J. D. CRAIG and A. D. SNEYD
University of Waikato, Private Bag 3105, Hamilton, New Zealand
(e-mail: math0097@waikato.ac.nz, sneyd@waikato.ac.nz)

(Received 3 March 2005; accepted 18 July 2005)

Abstract. To illustrate his theory of coronal heating, Parker initially considers the problem of disturbing a homogeneous vertical magnetic field that is line-tied across two infinite horizontal surfaces. It is argued that, in the absence of resistive effects, any perturbed equilibrium must be independent of z. As a result random footpoint perturbations give rise to magnetic singularities, which generate strong Ohmic heating in the case of resistive plasmas. More recently these ideas have been formalized in terms of a magneto-static theorem but no formal proof has been provided. In this paper we investigate the Parker hypothesis by formulating the problem in terms of the fluid displacement. We find that, contrary to Parker's assertion, well-defined solutions for arbitrary compressibility can be constructed which possess non-trivial z-dependence. In particular, an analytic treatment shows that small-amplitude Fourier disturbances violate the symmetry $\partial_z = 0$ for both compact and non-compact regions of the (x, y) plane. Magnetic relaxation experiments at various levels of gas pressure confirm the existence and stability of the Fourier mode solutions. More general footpoint displacements that include appreciable shear and twist are also shown to relax to well-defined non-singular equilibria. The implications for Parker's theory of coronal heating are discussed.

1. Introduction

One of the most stimulating ideas in solar physics is Parker's theory of coronal heating (Parker, 1972). Parker begins by considering a uniform magnetic field $B_0\hat{\mathbf{z}}$ line-tied to rigid plates $z = \pm a$ which approximate "frozen in" conditions at the photosphere. Motions in the photosphere displace the field-line footpoints, and Parker argues that the perturbed field cannot relax to a smooth equilibrium unless the perturbations have some kind of symmetry or involve an ignorable co-ordinate. In *almost all cases* singularities in the form of current sheets must appear. This result is precisely stated as a "Magnetostatic Theorem" in Parker (1994), but no rigorous proof is given.

The Parker hypothesis has several important consequences. For example, in the solar corona, the field of a weakly resistive solar plasma might be expected to collapse to small length scales in response to small-scale migrations of the footpoints. It follows that motions due to say, turbulent buffeting, could lead to very strong current densities and significant resistive energy dissipation, possibly sufficient to heat the corona. This theory has generated an extensive literature over the years, but it remains controversial (Rosner and Knobloch, 1982; van Ballegooijen, 1985; Antiochos, 1990). A number of closely related ideas seem promising – for

example, that nano-flares may be responsible for heating coronal active regions – but unequivocal observational support for a *specific* magnetic heating model is noticeably lacking (Fisher *et al.*, 1998).

Since the publication of Parker's original formulation, several authors have demonstrated general classes of footpoint displacements from which a smooth equilibrium will ensue, for example van Ballegooijen (1985) and Zweibel and Li (1987). More recent work by Bogoyavelenskij (2000a) has shown that there exist families of exact global solutions of the equilibrium equations, but the significance of these has been questioned by Parker (2000) and re-argued by Bogoyavelenskij (2000b).

The above results appear to contradict the magnetostatic theorem, but Parker (1994) argues that "the known continuous equilibria involve either only weak deformation of the field from a uniform state or a symmetry degeneracy". Parker's present position seems to be that the hypothesis holds good provided that footpoint displacements are of *sufficient amplitude and complexity*. This caveat means that the magnetostatic theorem no longer admits a precise mathematical statement.

A weakness of all the counter-examples to Parker's theory cited above is that the stability of the equilibria has not been established. Since an unstable equilibrium is physically inaccessible, it is not sufficient to establish the existence of a solution that contradicts the Parker assertion. A true counter-example should demonstrate stability, for example, by showing that the system can relax dynamically to the proposed equilibrium. One aim of this paper is address this flaw in previous arguments.

It is interesting that Parker's mechanism contrasts with other rigorously-established mechanisms of current-sheet formation, in particular, those involving energy release at a magnetic neutral point (Syrovatskii, 1971). In the case of a magnetic X-point, *any* field perturbation which changes the magnetic topology, no matter how small, gives rise to a current sheet: the size of the perturbation simply determines the length of the sheet, at least to within limits set by the global geometry. In the X-point collapse there is a privileged point – the center of the X – which focuses weak global perturbations into highly localized, large current density disturbances close to the origin (Syrovatskii, 1981; Craig and McClymont, 1993). There are no privileged points, however, in Parker's "non-equilibrium" theory (van Ballegooijen, 1985). Nor does his mechanism require the large scale, orchestrated, twisting motions associated with say a kink instability. If Parker's arguments are correct then any non-trivial, random walk of the footpoints can be expected to provide strong current densities and significant Ohmic heating (Ruzmaikin and Berger, 1998).

In fact various attempts have been made to simulate the Parker mechanism numerically (see Section 6.9 Parker, 1994). There is some evidence that random footpoint motions in an initially homogeneous field can lead to appreciable rates of Ohmic dissipation as found by Mikic, Schnack, and van Hoven (1989). These authors state however, that "our numerical simulations indicate that the field is able to settle to a force-free equilibrium after every imposed footpoint displacement,

without the generation of current sheets". This work militates against the Parker mechanism but, in the absence of a well-defined numerical protocol for identifying current sheets, it cannot be regarded as a definitive demonstration. What is required are numerical procedures that can systematically examine the strength and morphology of current singularities. This is a crucial point to which we return in Section 3 when we consider magnetic equilibria constructed using a non-resistive Lagrangian relaxation scheme.

The present paper aims to examine aspects of Parker's magnetostatic theorem in more detail. Two distinct approaches are taken. In Section 2 we use an analytic Lagrangian approach, in which fluid displacements are the primary variables, to demonstrate that small footpoint displacements cause smooth perturbations of the initial field. Our formulation is similar to that of Bobrova and Syrovatskii (1979) and Zweibel and Li (1987) but we include the effects of arbitrary plasma pressure for both compact and non-compact regions of magnetic fluid. This analysis, although contradicting Parker's claim that smooth disturbances of the field $\delta\mathbf{B}$ should be independent of z, is not definitive since , as mentioned above, it fails to establish the stability of the equilibria. In Section 3 however, a complimentary analysis based on a Lagrangian numerical scheme is used to investigate the finite amplitude stability of arbitrary initial fields. Specifically, we perform a series of numerical experiments that demonstrate the existence and stability of solutions in the presence of appreciable footpoint shear and twist. In all cases the computations are systematically refined in an attempt to ensure full numerical convergence. In the case of a current singularity, however, convergence cannot occur: the maximum current density on the mesh will in fact diverge at a rate determined by the strength and geometrical structure of the singularity. In common with Longbottom *et al.* (1998), we find that current sheets can be present in certain solutions – but only for "illegitimate" footpoint displacements not confined to the interior of the computational domain.

2. Analytic Formulation of the Parker Problem

2.1. Introduction

In the original Parker problem a uniform, vertical magnetic field, threaded between two infinite horizontal planes, and line-tied at the footpoints, is subject to arbitrary small footpoint disturbances. A natural question is whether there exist smooth, well-behaved solutions in the neighborhood of the original equilibrium. According to Parker's original argument, only magnetic fields which satisfy $\partial_z \mathbf{B} = 0$ provide well-behaved solutions. Since the symmetry $\partial_z = 0$ is incompatible with imposing relative footpoint displacements between the two planes, Parker contends that equilibria deriving from footpoint motions must be non-smooth, involving current singularities.

In the present section we formulate the Parker problem in terms of the linearized force operator $\mathcal{F}(\boldsymbol{\xi})$ which is defined in terms of small displacements $\boldsymbol{\xi}$ of the field lines (Bernstein *et al.*, 1958). Similar linearized formulations have been given by other authors (e.g., Zweibel and Li, 1987) and of particular interest is the demonstration of Bobrova and Syrovatskii (1979) that singularities *can develop* for certain classes of (pressureless) equilibria. At first sight this result seems sufficient to annihilate the Parker opposition (e.g., van Ballegooijen, 1985; Zweibel and Li, 1987). However, as shown below, the result of Bobrova and Syrovatskii (1979) does not apply to Parker-type equilibria whether the plasma is pressureless or not.

2.2. Formulation in terms of the fluid displacement

We imagine a homogeneous slab of plasma sandwiched between infinite rigid plates $z = -\ell$ and $z = \ell$ permeated by a uniform magnetic field $\mathbf{B}_0 = B_0\hat{\mathbf{z}}$. Footpoint displacements are then applied and the perturbed magnetic field is written in the form,

$$\mathbf{B} = \mathbf{B}_0 + \mathbf{b}(x, y, z), \quad P = P_0 + p(x, y, z),$$

where P is the plasma pressure. Note that Parker considers only an incompressible plasma and treats the **B**-field and the plasma pressure as the primary physical variables. Here we generalize to plasmas of arbitrary compressibility and take fluid displacements as the basic physical variables.

Suppose that pressure variations are related to the density disturbances according to

$$\frac{\partial P}{\partial \rho} = c^2,$$

where c is the sound speed. For a polytropic gas of index γ we have the usual relation $\rho c^2 = \gamma P$ The incompressible limit is approached by letting $c \to \infty$, but we can also model the opposite limit of an arbitrarily compressible "cold" plasma by letting $c \to 0$.

We now express the pressure and magnetic field disturbances in terms of the vector $\boldsymbol{\xi}(x, y, z)$, which represents the displacement of fluid particle in the transition from initial state to final equilibrium. The induction and continuity equations provide the first-order variations

$$\mathbf{b} = \nabla \times (\boldsymbol{\xi} \times \mathbf{B_0}), \quad p = -\rho_0 c_0^2 (\nabla \cdot \boldsymbol{\xi}),$$

and so the equation for the perturbed equilibrium, $\mathcal{F}(\boldsymbol{\xi}) = 0$, takes the form

$$\frac{1}{\mu}(\nabla \times \mathbf{b}) \times \mathbf{B}_0 + \rho_0 c_0^2 \nabla(\nabla \cdot \boldsymbol{\xi}) = 0. \tag{1}$$

2.3. CARTESIAN EQUATIONS FOR THE DISPLACEMENT

We take the upper and lower fluid boundaries to be

$$z = \pm\ell,$$

and express the fluid displacement in terms of Cartesian components,

$$\boldsymbol{\xi}(x, y, z) = [f(x, y, z), g(x, y, z), h(x, y, z)]. \tag{2}$$

Since fluid particles cannot penetrate the footpoints the vertical component of the displacement must satisfy

$$h(x, y, -\ell) = h(x, y, \ell) = 0. \tag{3}$$

We non-dimensionalize lengths with respect to ℓ, magnetic fields with respect to B_0, and pressures with respect to the undisturbed pressure P_0. Equation (1) then gives for the (x, y) displacements

$$f_{xx} + f_{zz} + g_{xy} = \beta p_x \tag{4}$$

$$g_{yy} + g_{zz} + f_{xy} = \beta p_y \tag{5}$$

where f_x denotes $\partial f/\partial x$, etc., and

$$\beta = \frac{\mu_0 P_0}{B_0^2} = \frac{\mu_0 \rho_0 c_0^2}{\gamma B_0^2}$$

defines the ratio of plasma to magnetic pressure. The z-component implies $p_z = 0$ and so the pressure disturbance is independent of z – a result reflecting the fact that the linearized Lorenz force must be orthogonal to the equilibrium field $\mathbf{B}_0$. Since $p = -\gamma \nabla \cdot \boldsymbol{\xi}$ is the dimensionless pressure perturbation we see that

$$-\gamma(f_x + g_y + h_z) = p(x, y), \tag{6}$$

must hold for non-vanishing p with $h(x, y, -1) = h(x, y, 1) = 0$, from condition (3).

Finally we note that the magnetic field perturbation $\mathbf{b}$ involves only the (x, y)-displacements,

$$\mathbf{b} = (f_z, g_z, -f_x - g_y). \tag{7}$$

This form, which automatically satisfies $\nabla \cdot \mathbf{b} = 0$, remains well defined even for plasmas of negligible pressure. Observe that in the pressureless limit, formally obtained by letting $\beta p \to 0$, Equation (6) cannot be imposed since only disturbances perpendicular to the equilibrium field lines can be determined. In fact pressureless modes constructed by Zweibel and Li (1987) contradict Parker's argument that only solutions satisfying $\partial_z \mathbf{b} = 0$ are permitted (see for example Parker, 1979, p. 373). In the following analysis we give a general treatment valid for arbitrary footpoint displacements in plasmas of arbitrary compressibility, for both compact and non-compact regions of the (x, y) plane.

2.4. Fourier representation of the problem

To construct general solutions with gas pressure we take a double Fourier transform, writing

$$F(z, \mathbf{k}) = \frac{1}{2\pi} \int_{E_2} f(x, y, z) \exp(-i\mathbf{k} \cdot \mathbf{r})\, \mathrm{d}x\, \mathrm{d}y$$

where E_2 is the entire (x, y)-plane and

$$\mathbf{r} = (x, y, z), \quad \text{and} \quad \mathbf{k} = (k_1, k_2, 0),$$

is a wave-vector in the (x, y)-plane whose amplitude is given by $k^2 = k_1^2 + k_2^2$. The Fourier transforms $G(z, \mathbf{k})$ and $H(z, \mathbf{k})$ are defined similarly. Transforms of functions which are independent of z will be distinguished by using the upper bar notation. Thus the Fourier transform of the pressure is written,

$$\bar{p}(\mathbf{k}) = \frac{1}{2\pi} \int_{E_2} p(x, y) \exp(-i\mathbf{k} \cdot \mathbf{r})\, \mathrm{d}x\, \mathrm{d}y.$$

With these conventions Equations (4)–(6) reduce to a system of ordinary differential equations in z, namely

$$F'' - k_1^2 F - k_1 k_2 G = i k_1 \beta \bar{p}, \tag{8}$$

$$G'' - k_2^2 G - k_1 k_2 F = i k_2 \beta \bar{p}, \tag{9}$$

$$H' + i k_1 F + i k_2 G = -\frac{\bar{p}}{\gamma}, \tag{10}$$

where the dash indicates differentiation with respect to z.

Let us assume that the footpoint displacements are specified *a-priori*. Then $F(\pm 1, \mathbf{k})$ and $G(\pm 1, \mathbf{k})$ are given and what needs to be shown is that well-defined solutions can be constructed subject to the constraint $H(-1, \mathbf{k}) = H(1, \mathbf{k}) = 0$.

2.5. The general solution

The system is simplified by introducing the auxiliary functions

$$U = k_1 F + k_2 G, \qquad V = k_2 F - k_1 G, \tag{11}$$

which correspond to $k^2 F = k_1 U + k_2 V$ and $k^2 G = k_2 U - k_1 V$. We find that U and V must satisfy,

$$U'' - k^2 U = i k^2 \beta \bar{p}, \quad V'' = 0, \tag{12}$$

and that Equation (10) can now be written in the form,

$$H' = -iU - \frac{\bar{p}}{\gamma}. \tag{13}$$

The general solutions of Equations (12) are

$$U = -i\beta\bar{p} + \bar{a}\cosh(kz) + \bar{b}\sinh(kz), \qquad V = \bar{c}z + \bar{d} \tag{14}$$

where $\bar{a}$ and $\bar{b}$, $\bar{c}$ and $\bar{d}$ are arbitrary functions of (k_1, k_2).

Using Equation (13), and the first of Equation (14), and remembering that $H(-1) = 0$, we find that

$$H = -\theta(z+1)\bar{p} - \frac{i\bar{a}}{k}(\sinh(kz) + s_k) - \frac{i\bar{b}}{k}(\cosh(kz) - c_k), \tag{15}$$

where we have introduced the abbreviations

$$\theta = \beta + \frac{1}{\gamma} \qquad c_k = \cosh(k), \quad s_k = \sinh(k).$$

The condition that $H(1) = 0$ shows that

$$\bar{p} = -\frac{i\bar{a}\, s_k}{\theta k}, \tag{16}$$

and substituting Equation (16), into Equations (15) and (14) we find,

$$U = -\frac{\bar{a}\,\beta s_k}{\theta k} + \bar{a}\,\cosh(kz) + \bar{b}\,\sinh(kz), \tag{17}$$

$$H = -\frac{i\bar{a}}{k}\,(\sinh(kz) - zs_k) - \frac{i\bar{b}}{k}(\cosh(kz) - c_k). \tag{18}$$

The arbitrary constants $\bar{a}$, $\bar{b}$, $\bar{c}$, and $\bar{d}$ are determined by the prescribed displacement on the boundaries $z = \pm 1$. It is simplest to work with the Fourier transforms of the auxiliary variables – that is $U(\pm 1, \mathbf{k})$ and $V(\pm 1, \mathbf{k})$ – which we write as

$$U(\pm 1, \mathbf{k}) = \bar{u}_\pm, \quad V(\pm 1, \mathbf{k}) = \bar{v}_\pm.$$

We find that

$$\bar{a} = \frac{\bar{u}_+ + \bar{u}_-}{2c_k + 2s_k\beta/k\theta}, \quad \bar{b} = \frac{\bar{u}_+ + \bar{u}_-}{2s_k}. \tag{19}$$

$$\bar{c} = \frac{\bar{v}_+ - \bar{v}_-}{2}, \quad \bar{d} = \frac{1}{2}(\bar{v}_+ + \bar{v}_-). \tag{20}$$

These relations confirm that arbitrary footpoint displacements lead to a well-defined Fourier representation of the solution.

It is interesting to note that only by assuming $U \equiv 0$ can we obtain modes consistent with Parker's claim that $\partial_z \mathbf{b} = 0$. This point is reinforced below when we specialize to discrete Fourier modes localized within compact regions of (x, y) plane.

2.6. Discrete fourier modes

Suppose rigid wall conditions are imposed at the boundaries of the square $0 < x, y < L$. Then disturbances can be constructed using superpositions of the discrete modes

$$f = F(z)\sin(k_1 x)\cos(k_2 y), \quad g = G(z)\cos(k_1 x)\sin(k_2 y), \tag{21}$$

where the pressure and vertical displacement take the forms

$$p = p_k \cos(k_1 x)\cos(k_2 y), \quad h = H(z)\cos(k_1 x)\cos(k_2 y). \tag{22}$$

Displacements on the side walls vanish provided that $k_1 L = m\pi$ and $k_2 L = n\pi$ where m and n are natural numbers. Substituting Equations (21) and (22) into Equation (4), (5), and (6) we find that f, g, and p satisfy Equations (8), (9), and (10) with ip replaced by $\bar{p}$. Repeating the analysis of Section 2.5 we find that f, g, and p represent a discrete mode with

$$p_k = -\frac{a_1 s_k}{\theta k}, \quad H(z) = \frac{a_1}{k}(s_k z - \sinh(kz)) - \frac{a_2}{k}(\cosh(kz) - c_k).$$

where $F(z)$ and $G(z)$ are defined, as previously, by the auxiliary functions

$$U = \beta p_k + a_1 \cosh(kz) + a_2 \sinh(kz), \quad \text{and} \quad V = a_3 + a_4 z.$$

Each mode is thus specified by four numbers a_1 to a_4, which determine the displacements on the upper and lower plates. This description also holds in the case of an incompressible plasma (see the Appendix).

As already mentioned, the simplest pressureless modes determine only the x and y components of the displacement. A typical field line associated with a low frequency mode $k_1 = 1, k_2 = 2$ is shown in Figure 1. Both footpoints of the initial line $x = 1,\ y = 1$ are significantly displaced ($a_1 = 0, a_2 = 0.3, a_3 = 0.05, a_4 = 2$). Figure 2 shows a pressureless two-mode superposition in which a $k \simeq 20$ mode is superposed with a $k \simeq 2$ displacement. We see that a narrow transition layer develops in the vicinity of the upper plate. This behavior is most simply understood by considering displacements which vanish on the lower plane $z = -1$. Setting $V = 0$ to eliminate the symmetry $\partial_z \mathbf{b}$ we find that

$$U \to a_1 \cosh(kz) + \frac{c_k}{s_k}\sinh(kz)$$

which is consistent with an exponential fall-off in distance s from the upper surface of the form $U \sim \mathrm{e}^{-ks}$. It follows that finite U contributions on the upper and lower plates can be expected to penetrate only a skin depth $s \sim k^{-1}$ into the interior $-1 < z < 1$.

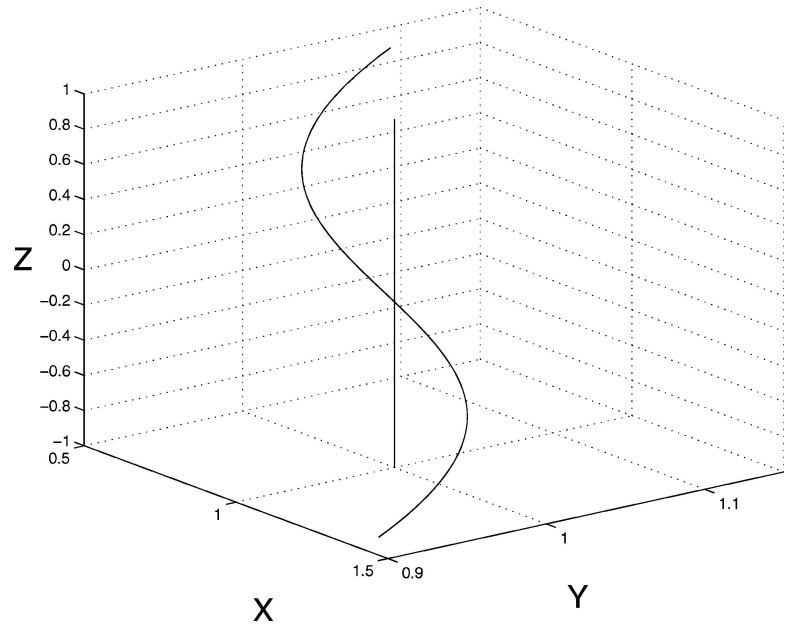

Figure 1. Distortion of a straight field line due to an individual Fourier mode ($k_1 = 1, k_2 = 2$) in a pressureless plasma. The plot is based on (21), and (22).

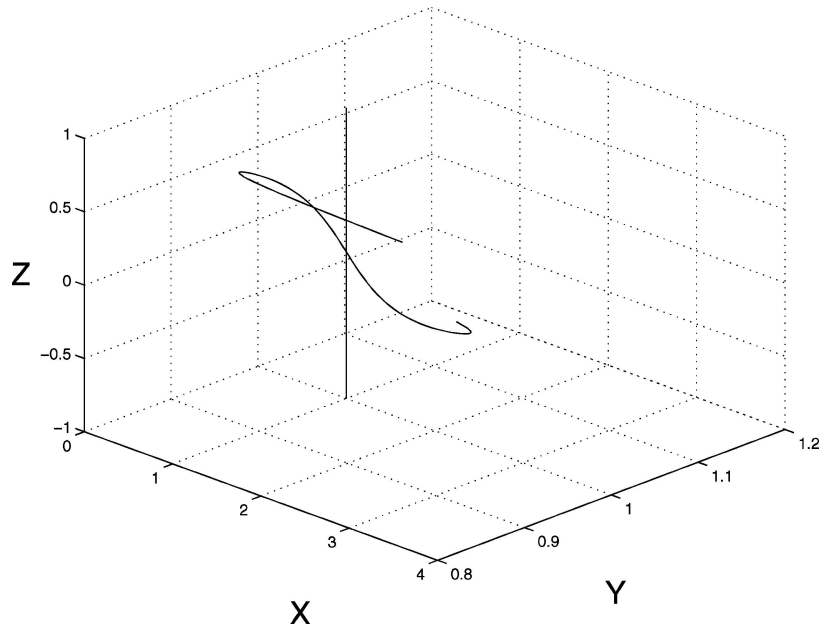

Figure 2. Field line plot based on the superposition of a high frequency ($k \simeq 20$) and a low frequency ($k \simeq 2$) Fourier mode. The strong distortion close to the upper plate $z = 1$ is a manifestation of the skin depth effect associated with high frequency behavior.

2.7. Discussion

The previous analysis makes it clear that linearized disturbances can be constructed to the Parker problem that violate the symmetry $\partial_z = 0$. Although this conclusion holds good for plasmas of arbitrary compressibility – and reinforces earlier analyses by van Ballegooijen (1985) and Zweibel and Li (1987) – it fails to deal a fatal blow to the Parker hypothesis. A complete rejection requires a proof of the existence *and stability* of equilibria that derive from arbitrary, finite amplitude displacements of the footpoints. This problem is explored using a computational Lagrangian approach in Section 3 below.

Despite this disclaimer, we know that the linearized approach is capable of predicting the formation of current singularities. Our formulation is similar to that of Bobrova and Syrovatskii (1979) who show that small boundary displacements of the pressureless field $\mathbf{B} = (\cos(\alpha z), \sin(\alpha z), 0)$ lead to singularities on surfaces defined by $k_1 \cos(\alpha z) + k_2 \sin(\alpha z)$ (where $\mathbf{k}$ is defined as above). It is clear however, that this initial field has considerably more structure than the homogeneous Parker field. The fields considered by Bobrova and Syrovatskii (1979) and Syrovatskii (1971) confirm that a collapse to singularity can be expected when the the background field includes distinct topological features such as nulls, separators (null–null lines), or mode rational surfaces, along which current naturally accumulates. However, since current sheets can also be formed by large-scale compressive or shearing motions in fields of little topological complexity (Low, 1987; Aly and Amari, 1989), there appears no universal criterion for the appearance of current singularities.

3. Magnetic Relaxation Experiments

3.1. Introduction

The existence and finite amplitude stability of solutions is conveniently explored using the magneto-frictional relaxation approach. This technique can be used both theoretically, in terms of thought experiments, and computationally, as a numerical relaxation scheme which preserves the field topology, to investigate ideal magnetic equilibria (e.g., Moffatt, 1985). In what follows we employ the Lagrangian code of Craig and Sneyd (1990) to realize 3D magnetic equilibria by the magneto-frictional method. This code provides a computational realization of the analytic Cauchy solution. The code has been well tested in a variety of applications (Longbottom *et al.*, 1998) and, unlike Eulerian schemes, has the advantage of working directly with the Lagrangian fluid displacements. The computational scheme is fully implicit and so time steps can be taken which exceed explicit thresholds by factors of 1000 or more. The code satisfies $\nabla \cdot \mathbf{B} = 0$ and identically conserves flux.

One difficulty with exploring the problem numerically, is that simulations are usually restricted to compact regions of space. In terms of the Parker problem,

we have seen in Section 2.6 that linearized Fourier modes can be constructed over compact regions of the (x, y) plane. It is convenient therefore to exploit these modes as prototype displacements for the initial magnetic relaxation experiment described below.

More generally, it should be recognized that finite amplitude displacements on the upper and lower plates must ultimately derive from footpoint motions involving a combination of rotation and shear. With this in mind we go on to perform a series of experiments incorporating successively more elaborate footpoint displacements.

3.2. FINITE AMPLITUDE SIMULATIONS

We determine solutions over the cube $-1 \leq x, y, z \leq 1$. A uniform distribution of fluid particles, of resolution $\Delta = 1/N$, is associated with the initial equilibrium $\mathbf{B} = \hat{\mathbf{z}}$. This distribution is distorted by imposing field line displacements on the boundaries based on Equation (21),

$$\Delta x = a \sin(m\pi x) \cos(n\pi y) z, \quad \Delta y = a \cos(m\pi x) \sin(n\pi y) z,$$

where a is an arbitrary amplitude. Fluid particles on the upper and lower plates are fixed by the initial conditions for all time, but particle slippage is allowed on the side walls where field lines do not penetrate.

The magnetic and pressure forces induced by the disturbance drive frictional fluid motions which remove energy from the fluid. In practice, we adopt the fictitious dimensionless equation

$$\mathbf{f} \equiv \nu \mathbf{v} = \mathbf{J} \times \mathbf{B} - \nabla P$$

where $\nu \simeq 1$ is the frictional coefficient and $P = \beta \rho^{\gamma}$. This equation compromises neither the final equilibrium $\mathbf{f} = \mathbf{v} = 0$ nor its stability. Therefore, subject only to the condition that the numerical resolution is adequate, the magneto-frictional method guarantees a stable relaxed solution. The present simulations have all been run to full convergence, a point we emphasize in Section 3.4 below, and tested for comparison with the analytic treatment of Section 2.6 in the case of weak displacements $a \ll 1$.

Figure 3 shows raw data from a typical run at modest resolution ($a = 1, m = 1, n = 2, \beta = 0.05, \gamma = 1, N = 20$). Fluid particles lie at the intersections of the mesh and these delineate near vertical field lines which thread the lower and upper plates. In Figure 3a we display an $x = 0$ mesh slice and it is clear that, consistent with the linear analysis, the bulk of the mesh distortion occurs in the horizontal boundary layers close to the upper and lower plates. Field lines are also sheared across the $y = 0$ plane as indicated by Figure 3b. The symmetry of the disturbance ensures that the particles initially in the plane $z = 0$ move only in the vertical direction. Figure 3c and d show the fixed meshes associated with the footpoints displacements on $z = \pm 1$.

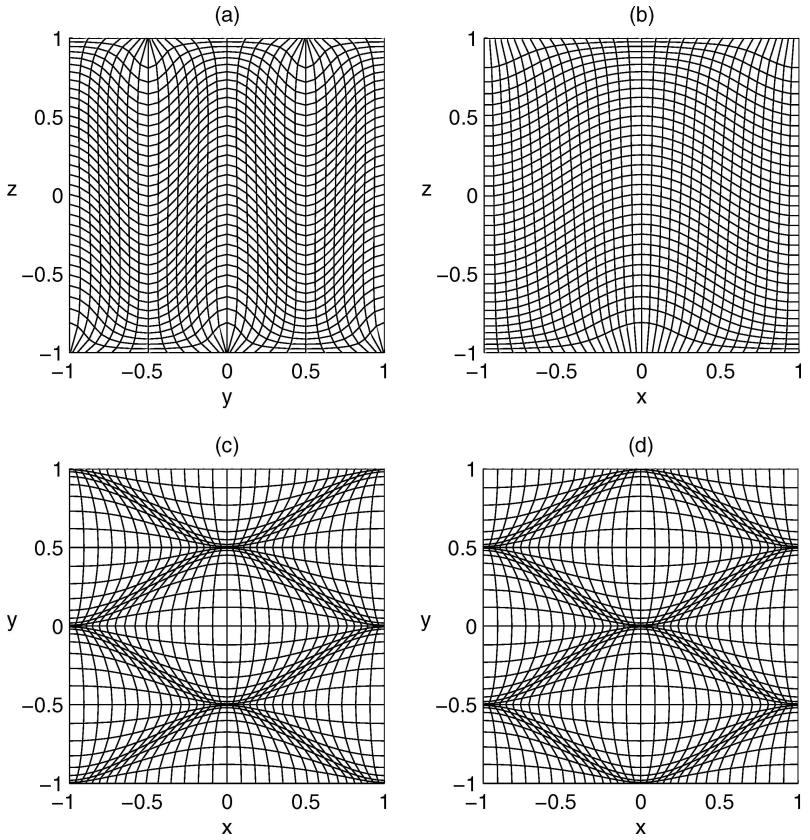

Figure 3. Equilibria obtained by imposing finite amplitude footpoint displacements on the initial Parker field defined over the cube $-1 < x, y, z < 1$. Figure 3a shows an $x = 0$ slice of the Lagrangian mesh for $N = 16$. Fluid particles are constrained to field lines defined by the initial Parker field. Traversing the upper and lower plates are near vertical lines that trace magnetic field lines in the relaxed equilibrium. Figure 3b shows the corresponding $y = 0$ surface. Upper and lower footpoint displacements are shown in Figures 3c and d, respectively.

The shearing and compression of the fluid that derives from the initial disturbance imparts only a modest degree of twist to the field. This twist represents magnetic helicity which is identically conserved in the relaxation. The inherent twist is particularly clear from the isosurface plot of the relaxed current density in Figure 4. The current surfaces form a periodic array of twisted and elongated "hourglass" figures. Most of the current is associated with the footpoints, but there is a central narrow shard that penetrates the central $z = 0$ surface.

3.3. SOLUTIONS INVOLVING ORCHESTRATED TWIST

The global displacements considered so far have been motivated by the linear analysis of Section 3. Such low frequency, isolated modes do not impart a large scale

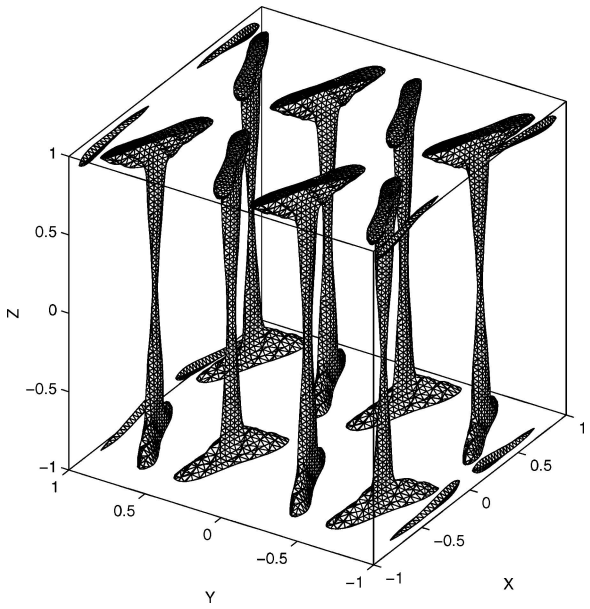

Figure 4. Current density isosurfaces in the relaxed equilibria of Figure 3. The periodic structure reflects the symmetry of the initial, finite amplitude, Fourier displacement ($k_1 = 1, k_2 = 2$). Note that to obtain good definition of the isosurfaces a slightly higher resolution than that of Figure 3 was used, namely $N = 28$.

rotation to the initial field and only by a complicated superposition of many such modes can orchestrated twisting motions be modeled. In the relaxation experiment performed below we apply a rotation directly to the footpoints of the upper the lower plates.

Figure 5 illustrates the results of a relaxation experiment in which field lines wind through roughly one turn in traversing the plates $z = -1$ to $z = +1$. The initial condition is based on a uniform planar mesh (x, y) which is twisted according to

$$x \to x\cos\phi - y\sin\phi \qquad y \to x\sin\phi + y\cos\phi,$$

where

$$\phi = \phi(x, y, z) = zf(x, y),$$

and $f(x, y)$ is chosen to fall off smoothly with distance from the rotation axis $x = y = 0$. This form of highly non-linear disturbance leads to identical $x = 0$ and $y = 0$ slices (left-hand figure)) and to opposing rotations on the upper and lower plates (right-hand figure).

Despite the appreciable degree of applied twist the final equilibrium (not shown) is not especially interesting, the current being concentrated in a single vertical column centered at the origin. The important point, as emphasized

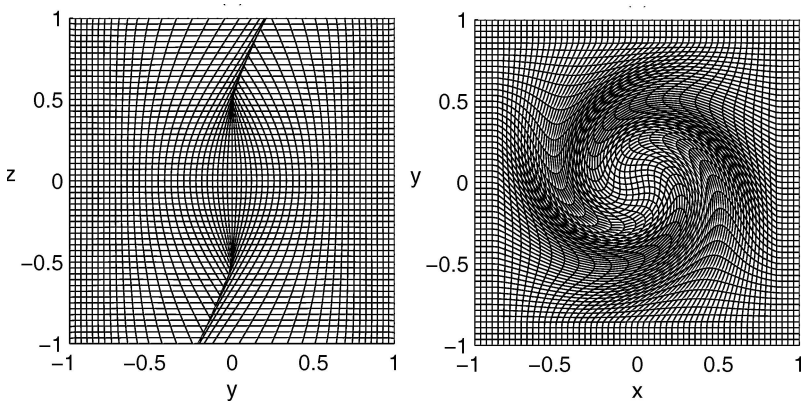

Figure 5. Equilibrium meshes that derive from large amplitude footpoint rotations of the initial field ($N = 28$). The figure on the left illustrates the mesh twisting associated with the $x = 0$ or $y = 0$ mesh slices. That on the right shows the footpoint displacements.

below, is that the solution converges convincingly as the numerical resolution is increased.

3.4. Convergence of numerical solutions

In the previous sections we have displayed relaxed equilibria at only modest resolution. However, if current singularities were forming – and remember that we impose footpoint displacements that break the symmetry $\partial_z = 0$ of the initial field – then we would expect the maximum current density on the mesh to grow systematically with increasing resolution. Yet, as the two lower plots of Figure 6 confirm, the two numerical equilibria represented above are fully converged for $N \simeq 30$. Notably the convergence pattern remains identical as the differential rotation of the footpoints is increased (see upper plots of Figure 6). The implication is that the well-behaved, smooth equilibria are determined by the relaxation scheme for each of the non-linear footpoint disturbances.

It is important to emphasize that the ability of the present Lagrangian scheme to model current singularities has been tested repeatedly in a variety of applications (see Craig and Sneyd, 1990; Longbottom *et al.*, 1998). For example, it is easy to show using flux conservation arguments (see the Appendix of Ali and Sneyd, 2002), that the current density associated with an idealized singularity should increase as

$$J_{\max} = AN^{\alpha} \tag{23}$$

where α is typically a positive number of order unity and A a constant. The exact speed of the blow-up depends in fact on the nature of the magnetic collapse, for instance, whether the singularity is compressional or rotational. If compressional,

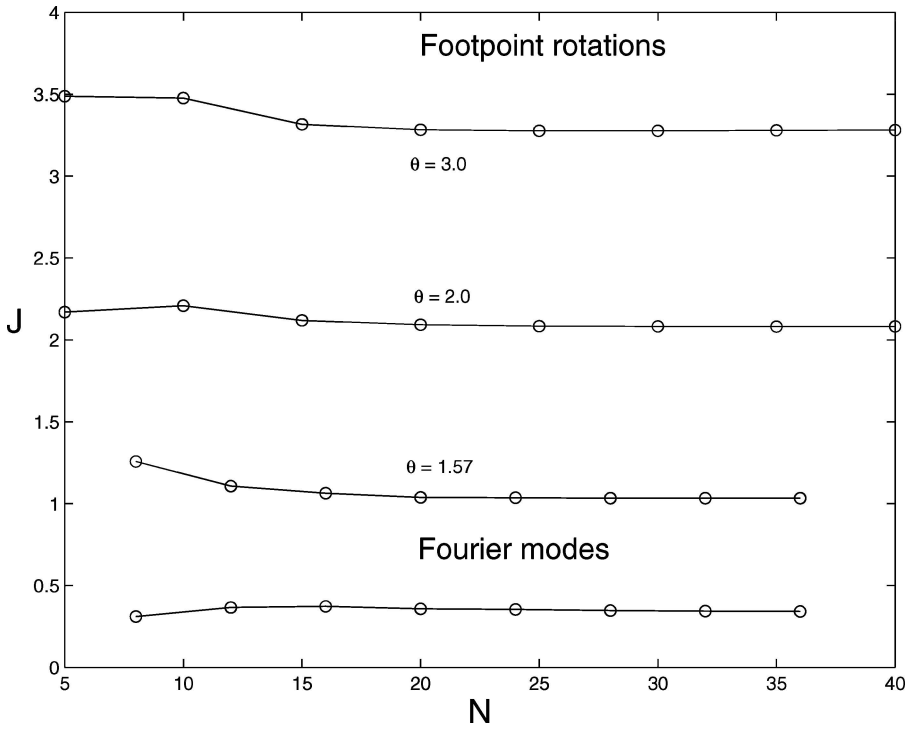

Figure 6. Convergence of the current density J with number of grid points N for each of the magnetic relaxation experiments. The upper curves plot the maximum current density over the mesh for the footpoint rotation experiment of the figure. The angle θ represents the differential rotation between the upper and lower plates in radians. The lower curve gives the maximum current density for the finite-amplitude Fourier mode disturbance of Figure 3.

the blow-up will depend on the amplitude of the gas pressure, that is $\alpha = \alpha(\beta)$ (Craig and Litvinenenco, 2005). But in all cases, and in marked contrast to the results of Figure 6, the ideal singularity is manifested by the systematic increase in current density with resolution.

3.5. Solutions involving rotation and shear

By applying a succession of rotation and shearing motions very complicated footpoint displacements can be constructed. The price paid for this extra complexity is the increased time for numerical convergence. In the examples considered below (the convergence pattern of Figure 6), the convergence does not set in until typically $N \simeq 40$.

Our first example is that of two flux tubes twisted around each other. To construct such a field two localized twists of opposite sense were applied to produce two twisted flux tubes. Then a global twist was applied to wrap the tubes around

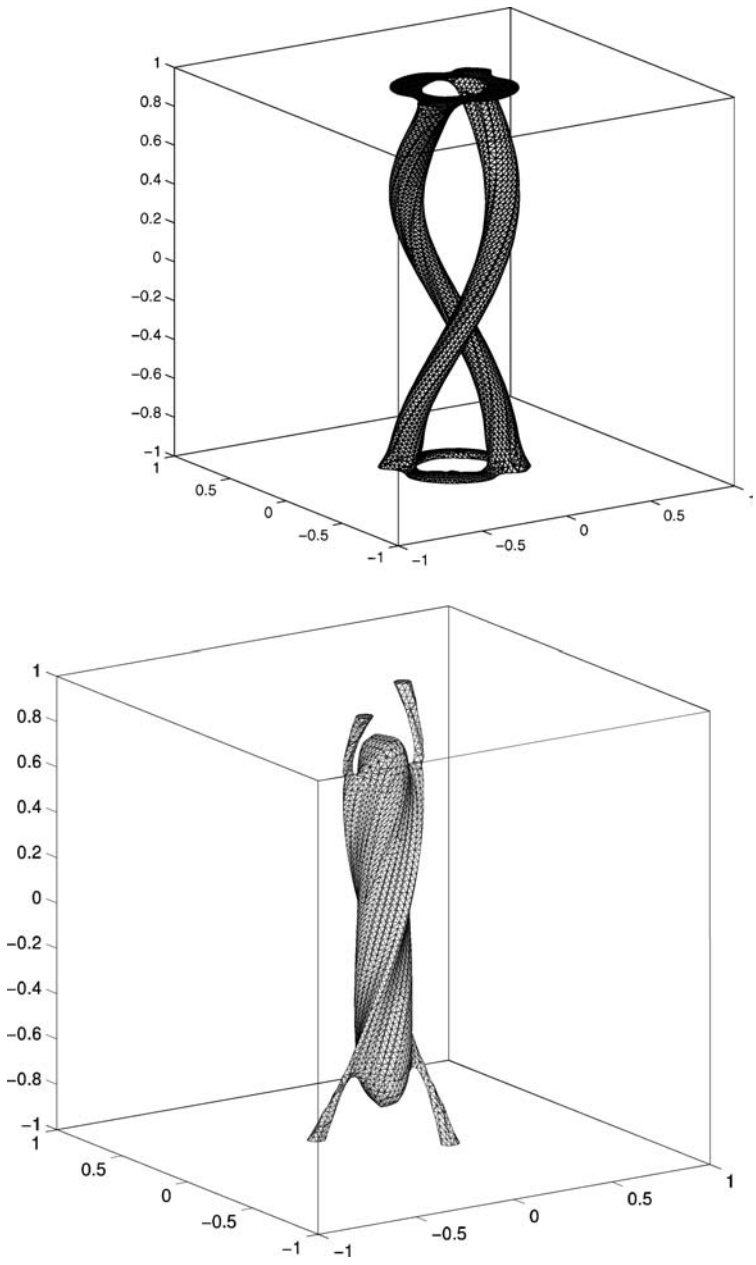

Figure 7. Current isosurfaces: upper figure, the initial state, and lower, the final relaxed state.

each other, as illustrated in Figure 7. Although this configuration is very similar to that suggested by Parker (1994) we detected no tendency for intense current growth during relaxation to equilibrium. The relaxed current iso-surface shows that the initial twisted tubes of current eventually degenerate into vestigial strands

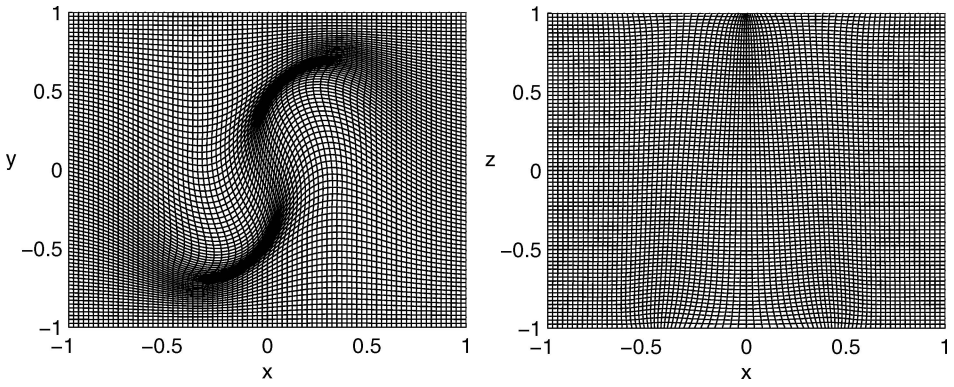

Figure 8. Initial footpoint displacement for twist and shear combination.

encircling the strong central column formed by the overall large-scale rotation. In our second example we apply a combination of both shear and twist, giving the footpoint displacement shown in Figure 8. Again, despite experiments with varying combinations of shear and rotation, we found no evidence of current-sheet formation.

3.6. Rotational boundary displacements

So far we have considered footpoint displacements which are irrotational or vanish on the lateral boundaries $x = \pm 1$, $y = \pm 1$ – i.e., which result in a zero component of $\nabla \times \mathbf{B}$ perpendicular to the boundary. Allowing displacements with a non-zero component of $\nabla \times \mathbf{B}$ effectively drives an electric current across the boundary, changing the results significantly. For example, Longbottom *et al.* (1998) performed relaxation experiments in which the boundary points were sheared in both directions, resulting in a normal component of $\nabla \times \mathbf{B}$, and evidence of current-sheet formation was found.

Motivated by Longbottom *et al.* (1998), we now perform an experiment using initial boundary displacements of the form,

$$x = x + s_x\, xz(1 - x^2)^2, \quad y = y + s_y\, xz(1 - y^2)^2,$$

where s_x and s_y represent the magnitudes of the shears in the x and y-directions respectively. Graphs illustrating the convergence or divergence of the current density with zero gas pressure are shown in Figure 9. For relatively small shears there is no evidence of a current sheet, the maximum current settling down to a constant value. However for shears greater than about $s = 0.2$ we find evidence of current-sheet formation, the maximum current growing with increasing resolution. For a shear of magnitude $s = 0.6$ the asymptotic growth rate with resolution of $J_{\max}$

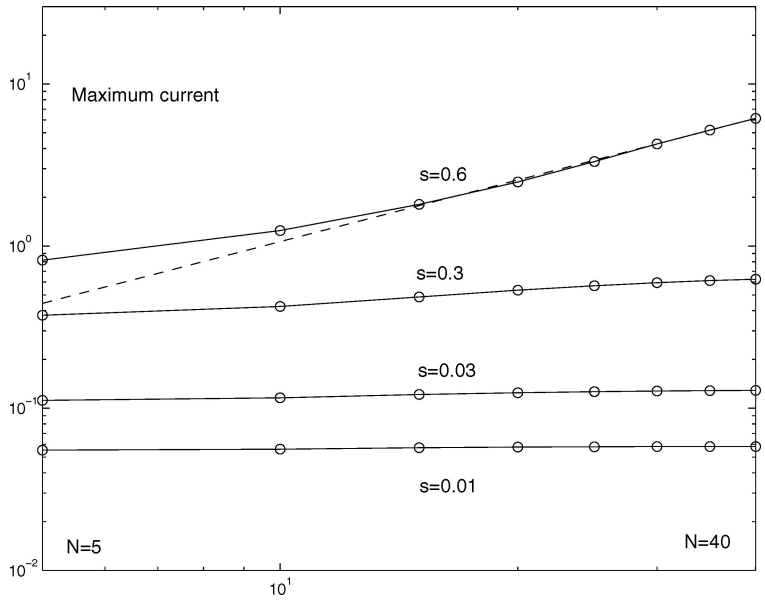

Figure 9. Graphs of maximum current $J_{\max}$ versus number of grid points N for a variety of shear strengths. Plasma pressure is neglected. The dashed line represents asymptotic current growth in the case $s = 0.6$ of power-law slope 1.263.

approximates a power law (23), of amplitude $A = 5.812$ and exponent $\alpha = 1.263$. As already mentioned, such power-law growth is expected in the presence of a current sheet (Ali and Sneyd, 2001). These results show that the current singularities found by Longbottom *et al.* (1998) are a nonlinear phenomenon in which the results depend crucially on the amplitude of the initial perturbation. Such results cannot of course be revealed by linear analysis. Figure 10 shows results of a similar experiment with gas pressure $\beta = 0.1$. Again, there is evidence of current-sheet formation, but the asymptotic growth rate is slowed somewhat to $\alpha = 0.851$. Independent calculations (Craig and Litvinenenco, 2005) indeed confirm that gas pressure can be expected to weaken the current singularity, but cannot suppress it entirely.

But to what extent can disturbances extending to the lateral boundaries of the model be regarded relevant to the validity of the Parker hypothesis? It seems to us that the injection of electric current normal to the direction of initial field is an additional effect, not part of the original Parker scenario. If we assume that we are searching for an effect that is robust to the prescription of the lateral boundaries, then such boundaries should be placed well away from the regions of appreciable footpoint motion. With this interpretation, the singular equilibria presented here, along with those of Longbottom *et al.* (1998), should not be taken as evidence in support of the Parker hypothesis.

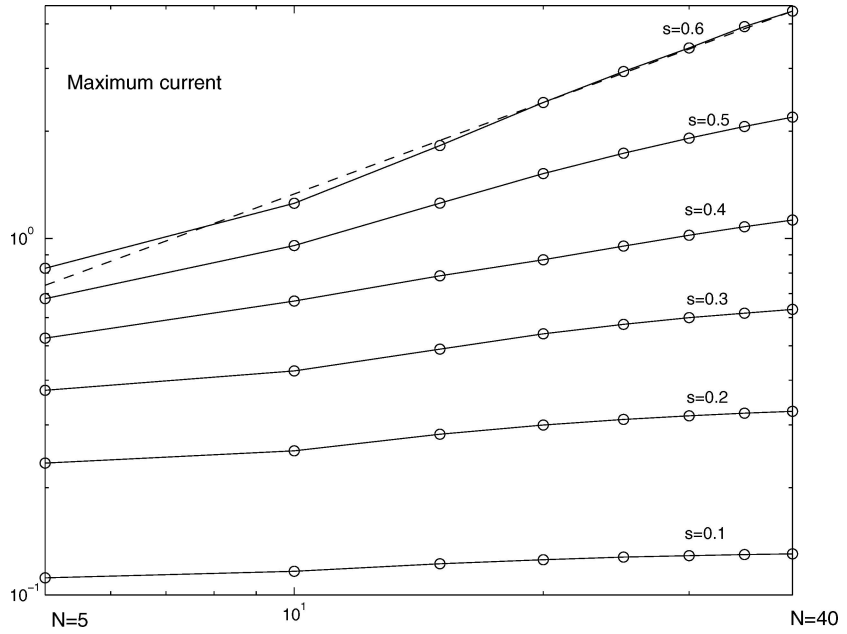

Figure 10. Graphs of maximum current 0.1. $J_{\max}$ versus number of grid points N for a variety of shear strengths s. The plasma pressure $\beta = 0.1$. The dashed line represents asymptotic current growth in the case $s = 0.6$ of power-law slope 0.851.

4. Discussion and Conclusions

We have considered the Parker problem for the case of arbitrary footpoint displacements in an ideal, compressible plasma. An analytic treatment of the linearized problem, based on the Lagrangian formulation of Bernstein *et al.* (1958) shows that equilibrium solutions can be constructed for all footpoint disturbances. These solutions violate the symmetry $\partial_z \mathbf{B} = 0$ (in agreement with van Ballegooijen, 1985; Zweibel and Li, 1987) which is an essential feature of Parker's argument, yet leads to smooth, well-behaved equilibria. In particular, if those modes which lead to z-independent field perturbations are eliminated, then boundary disturbances penetrate only weakly into the interior volume. For a planar wavenumber k we find that perturbations die away according to the skin depth formula $\exp(-ks)$ where s is the distance from the boundary. The penetration of a general disturbance is therefore controlled mainly by the fundamental modes of the problem and, in practice, these will be determined by the radial and vertical length scales of the equilibrium field. These findings are robust to the plasma compressibility (see the Appendix) and hold good, no matter whether a compact or unbounded planar region is considered.

Of course, as we have emphasized, the linear analysis by itself is not sufficient to negate Parker's coronal heating hypothesis. The problem of stability needs to be addressed and, in particular, the impact of finite-amplitude disturbances. In view of the nonlinear, three-dimensional nature of the general stability problem we have used the non-resistive Lagrangian code of Craig and Sneyd (1990) (see also Longbottom *et al.*, 1998) to explore computationally the properties of line-tied $\mathbf{B} = \hat{\mathbf{z}}$ equilibria. For appreciable footpoint displacements, even those involving significant orchestrated twist, it is possible to obtain fully converged numerical results. Such smooth behavior, while extending and reinforcing the linear analysis, directly contradicts Parker's assertion of generic singular behavior in ideal MHD equilibria. In Section 3.6 we did manage, however, to obtain numerical behavior consistent with the emergence of current singularities. But this was achieved, in common with Longbottom *et al.* (1998), by manipulating the lateral boundaries of the computational domain, an exercise which does not seem legitimate in terms of the Parker hypothesis.

To what extent have we disproved Parker's argument? The linearized analysis shows that a collapse to singularity requires nonlinear footpoint disturbances, but it could be argued that the finite-amplitude displacements we have tested lack "sufficient amplitude and complexity". The disturbances we construct, based on finite amplitude rotation and shear are arbitrary but of course their amplitude and complexity must always be limited by the computing power available. Figure 6 does, however, provide some evidence that increasing the amplitude of the field-line rotations has little effect on the convergence of $\mathbf{J}$ to a finite value. The three results at increasing amplitude converge in a similar manner.

Yet by changing the "rules of the game" and allowing large-scale footpoint displacements that extend to the lateral boundaries of the model, we have been able to trigger a collapse to singularity using quite simple non-linear disturbances. This result, which agrees with Longbottom *et al.* (1998), suggests that the original Parker geometry may be less susceptible to small-scale "internal" footpoint migrations than to global, orchestrated disturbances. That is, only by a non-trivial change in the Parker formulation have we been able to witness evidence for current-sheet formation.

While the present arguments lend no support to Parker's magnetostatic theorem, they should not be taken to imply that random footpoint motions are incapable of heating the corona. What they do suggest is that, in the absence of topological features in the background field such as magnetic nulls or separators, appreciable footpoint migrations cannot generally be expected to induce a collapse to small length scales leading to current-sheet formation. Significant current densities may emerge, but unless large amplitude orchestrated motions are present, these will simply reflect the length scales associated with a random accumulation of footpoint displacements.

Acknowledgements

We are grateful to Stathie Triadis for his assistance with computations and preparation of diagrams. This work was partially supported by the Marsden fund, grant no. 02-UOW-050 MIS.

Appendix: Incompressible Solutions

In Parker's original formulation only an incompressible plasma is considered. Here we point out that incompressible solutions can be easily deduced from the compressible Lagrangian formulation presented here.

First note that an incompressible plasma requires that $\nabla\cdot\mathbf{u} = \nabla\cdot\boldsymbol{\xi} = 0$. Suppose p_i is the (incompressible) pressure amplitude that achieves this requirement. From Equation (10) we see that for γ fixed we must let $\bar{p} \to 0$ to obtain $\nabla\cdot\boldsymbol{\xi} \to 0$. A finite pressure amplitude then requires the identification $p_i = \beta\bar{p}$ in the limit $\beta \to \infty$. It follows that incompressibility is achieved by the replacements $\theta \equiv \beta + 1/\gamma \to \beta,\ p_i \to \beta\bar{p}$.

As a simple example consider the incompressible $\beta \to \infty$ limit for the discrete Fourier modes of Section 2.6. We write $p = p_i \cos(k_1 x)\cos(k_2 y)$, set $U = p_i + a_1\cosh(kz) + a_2\sinh(kz),\ \theta = \beta$, and take $p_i = -a_1 s_k/k$. All other expressions are unchanged. Similar replacements go through for the Fourier integral solutions of Section 2.5.

References

Ali, F. and Sneyd, A.: 2001, *Geophys. Astrophys. Fluid Dyn.* **94**(3–4), 221.
Ali, F. and Sneyd, A.: 2002, *Solar Phys.* **205**, 279.
Aly, J. and Amari, T.: 1989, *Astron. Astrophys.* **221**, 287.
Antiochos, S.: 1990, *Soc. Astron. Italiana* **61**, 369.
Bernstein, I., Frieman, E., Kruskal, M., and Kulsrud, R.: 1958, *Proc. R. Soc. Lond.* **244**, 17.
Bobrova, N. and Syrovatskii, S.: 1979, *Solar Phys.* **61**, 379.
Bogoyavelenskij, O.: 2000a, *Phys. Rev. Lett.* **84**, 1914.
Bogoyavelenskij, O.: 2000b, *Phys. Rev. Lett.* **85**, 4406.
Craig, I. and Litvinenenco, Y.: 2005. *Phys. Plasmas* **12**, 032301.
Craig, I. and McClymont, A.: 1993, *Astrophys. J.* **405**, 405.
Craig, I. and Sneyd, A.: 1990, *Astrophys. J.* **357**, 653.
Fisher, G., Longcope, D., Metcalf, T., and Petsov, A.: 1998, *Astrophys. J.* **508**, 885.
Longbottom, A., Rickard, G., Craig, I., and Sneyd, A.: 1998, *Astrophys. J.* **500**, 471.
Low, B.: 1987, *Astrophys. J.* **323**, 358.
Mikic, Z., Schnack, D., and van Hoven, G.: 1989, *Astrophys. J.* **338**, 1148.
Moffatt, H.: 1985, *J. Fluid Mech.* **159**, 359.
Parker, E.: 1972, *Astrophys. J.* **174**, 499.

Parker, E.: 1979, *Cosmical Magnetic Fields, Their Origin and Activity*, The International Series of Monographs on Physics, Clarendon, Oxford.
Parker, E.: 1994, *Spontaneous Current Sheets in Magnetic Field*, Oxford University Press, New York, Oxford.
Parker, E.: 2000, *Phys. Rev. Lett.* **85**, 4405.
Rosner, R. and Knobloch, E.: 1982, *Astrophys. J.* **262**, 349.
Ruzmaikin, A. and Berger, M.: 1998, *Astron. Astrophys.* **337**, L9.
Syrovatskii, S.: 1971, *Sov. phys. JETP* **33**, 933.
Syrovatskii, S.: 1981, *Ann. Rev. Astron. Astrophys.* **19**, 163.
van Ballegooijen, A.: 1985, *Astrophys. J.* **298**, 421.
Zweibel, E. and Li, H.-S.: 1987, *Astrophys. J.* **312**, 423.